J. Fluid Mech. (1996), *vol.* 316, *pp.* 241–257

Boundary-layer flow around a submerged circular cylinder induced by free-surface travelling waves

By B. YAN AND N. RILEY

School of Mathematics, University of East Anglia, Norwich, NR4 7TJ, UK

(Received 21 August 1995 and in revised form 8 February 1996)

We consider the fluid flow induced when free-surface travelling waves pass over a submerged circular cylinder. The wave amplitude is assumed to be small, and a suitably defined Reynolds number large, so that perturbation methods may be employed. Particular attention is focused on the steady streaming motion, which induces circulation about the cylinder. The viscous forces acting on the cylinder are calculated and compared with the pressure forces which are solely responsible for the loading on the cylinder in a purely inviscid flow.

1. Introduction

In this paper we consider the flow induced in an incompressible, viscous fluid when monochromatic free-surface waves propagate over a submerged circular cylinder whose generators are parallel to the wave crests. The dimensionless wave amplitude ϵ is assumed to be small, whilst a suitably defined Reynolds number R_s is assumed to be large, so that perturbation techniques may be used in the solution construction. The study relates to the practical areas of flow about the horizontal pontoons of semi-submersibles and tension-leg platforms, and wave energy devices.

For an inviscid fluid the earliest work by Dean (1948), based on the conformal mapping technique, showed that at leading order, $O(\epsilon)$, there is no reflection of the incident waves. This result was confirmed by Ursell (1950), using a series of multipole potentials, from which complete details of the flow may be inferred. Subsequently Vada (1987) obtained both the first- and second-order diffraction potentials numerically using a method based on Green's second identity and a special Green's function given by Wehausen & Laitone (1960). Vada showed, in particular, that Dean's result of zero reflection coefficient extends to second order also, within the accuracy of his numerical method. This particular point was subsequently addressed by McIver & McIver (1990) and Wu (1991). Both note that the second-order reflection coefficient R_2 may be expressed in terms of the first-order potential. McIver & McIver then show analytically that $R_2 \equiv 0$, whilst Wu achieves the same result numerically. Riley & Yan (1996) have confirmed the results of Vada (1987) for the first- and second-order diffraction problems, using a different numerical method, and have completed the second-order solution by including the time-independent contribution. Meanwhile, in a series of papers, Chaplin (1984*a*,*b*, 1992, 1993) has studied by both experimental and theoretical means the flow of a real fluid in configurations relevant to the present work. The earlier papers, Chaplin (1984*a*,*b*) are largely experimental, with a circular cylinder located beneath a free surface over which waves travel. The mass transport

flow around the cylinder is investigated, Chaplin (1984*a*), using flow visualization. For the cylinder at relatively large depth, good agreement with a theory that invokes the streaming velocity at the edge of the Stokes layer, formed on the cylinder surface, is obtained. In a second paper, Chaplin (1984*b*), the forces acting on the cylinder are measured. No detectable reflection at either second or third order in wave amplitude was detected, and the dominant nonlinear component of force acting on the cylinder was shown to be of third order in wave amplitude. More recently Chaplin (1992) has considered the general orbital flow about a circular cylinder, using boundary-layer techniques introduced by Stuart (1966) and Riley (1965, 1967). In an application to our title problem he acknowledges the need to introduce a potential vortex flow outside boundary layers at the cylinder surface, and approximates this by a classical, bound, vortex located at the centre of the cylinder. His most recent paper, Chaplin (1993), attacks the problem of uniform circular orbital flow in the presence of a circular cylinder at finite Reynolds number using the full Navier–Stokes equation. In the higher Reynolds number regime good agreement with a boundary-layer theory of Riley (1971) is recorded. The same problem is addressed by Stansby & Smith (1991), using the random vortex method.

There is a sense in which Chaplin's (1992) work anticipates that presented here. As already indicated, we assume that the incident wave amplitude is small and that the streaming Reynolds number is large so that boundary-layer techniques may be used, and a completely rational theory developed. Section 2 establishes the appropriate equations, and well-established techniques are used in §3 to develop a perturbation solution. In particular the steady streaming within the Stokes layer, thickness $O(\epsilon/R_s^{1/2})$, is determined. Most attention is focused on the flow in an outer boundary layer, thickness $O(R_s^{-1/2})$, of steady streaming. In this outer boundary layer it is established that vorticity is transported by the Lagrangian, not Eulerian, mean velocity. The flow in the boundary layers induces a circulation about the cylinder, and a bound vortex is introduced that satisfies conditions not only at the cylinder surface, but also at the mean position of the free surface. The circulation associated with this vortex has to be determined with care, ensuring that the boundary-layer vorticity matches correctly with the (irrotational) outer flow. The technique adopted is described in detail by Riley (1981). The forces acting on the cylinder are determined. The normal stress is dominated by the pressure, leading to a fluctuating component with the fundamental frequency at $O(\epsilon)$ and a second harmonic, together with a time-averaged component, at $O(\epsilon^2)$. The latter is a lift force, with no drag, on the cylinder. These results are in accord with those of Vada (1987). Viscous effects contribute to the pressure an unsteady term $O(\epsilon^2/R_s^{1/2})$, with the fundamental frequency, which is small and not calculated explicitly. Viscous effects are also responsible for a circulation about the cylinder, contributing an unsteady term $O(\epsilon^3)$ to the pressure. Since the experiments of Chaplin (1984*b*) detect a strong third-order component in the fluctuating force we have calculated this contribution explicitly. The viscous shear stresses also have fluctuating contributions with both the fundamental and second harmonic frequencies, together with a time-independent part, all of which are smaller than their pressure-force counterparts by a factor $O(\epsilon/R_s^{1/2})$. We note that the time-averaged shear stress augments the lift force and also contributes a 'drag' force in the direction of propagation of the incident wave.

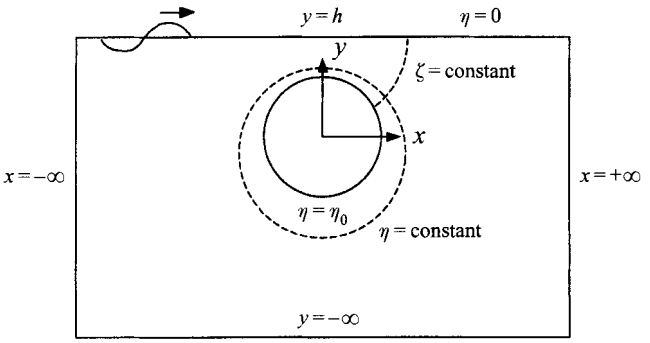

FIGURE 1. Definition sketch.

2. Governing equations

Two-dimensional monochromatic waves propagate at the surface of an incompressible, viscous fluid of infinite depth over a submerged circular cylinder; the wave crests are parallel to the generators of the cylinder, see figure 1. If a is the radius of the cylinder, A, ω the amplitude and frequency of the incident waves respectively, then with a as a typical length, ω^{-1} a typical time and $U_0 = a\omega$ a velocity the non-dimensional equation for the stream function ψ may be written as

$$\frac{\partial(\nabla^2\psi)}{\partial t} - \frac{1}{r}\frac{\partial(\psi, \nabla^2\psi)}{\partial(r,\theta)} = \frac{\epsilon^2}{R_s}\nabla^4\psi, \tag{2.1}$$

where

$$\nabla^2 = \frac{1}{r}\frac{\partial}{\partial r} + \frac{\partial^2}{\partial r^2} + \frac{1}{r^2}\frac{\partial^2}{\partial\theta^2}. \tag{2.2}$$

In these equations (r,θ) are polar coordinates with origin at the centre of the cylinder, and $\theta = 0$ coincident with the direction of propagation of the incident waves. The two parameters that characterize the flow are the Strouhal number ϵ^{-1}, and streaming Reynolds number R_s, defined as

$$\epsilon = \frac{A}{a}, \qquad R_s = \frac{A^2\omega}{\nu}, \tag{2.3}$$

where ν is the kinematic viscosity. The velocity components (v_r, v_θ) are defined in terms of the stream function as

$$v_r = \frac{1}{r}\frac{\partial\psi}{\partial\theta}, \qquad v_\theta = -\frac{\partial\psi}{\partial r}. \tag{2.4}$$

Equation (2.1) is to be solved subject to the following boundary conditions:

$$\frac{\partial\psi}{\partial\theta} = \frac{\partial\psi}{\partial r} = 0 \quad \text{at } r = 1, \tag{2.5}$$

$$\nabla\psi \to \mathbf{0} \quad \text{as } y \to -\infty, \tag{2.6}$$

together with suitable wave conditions as $x \to \pm\infty$, and free-surface conditions applied at the mean position of the free surface $y = h = H/a$, where H is the depth of the centre of the cylinder beneath the undisturbed position of the free surface. The coordinates (x, y) also have their origin at the centre of the cylinder.

3. Solution procedure

With $\epsilon \ll 1$ we expand the stream function as

$$\psi(\boldsymbol{x},t) = \epsilon\psi_1(\boldsymbol{x},t) + \epsilon^2\{\psi_2^{(u)}(\boldsymbol{x},t) + \psi_2^{(s)}(\boldsymbol{x})\} + \epsilon^3\psi_3(\boldsymbol{x},t) + \epsilon^4\psi_4(\boldsymbol{x},t)..., \tag{3.1}$$

where at $O(\epsilon^2)$ we have anticipated that the time-averaged or steady flow, denoted by superscript (s), is non-zero. Riley & Yan (1996) have considered the flow under investigation here for an inviscid fluid. The leading-order term ψ_1, first considered by Dean (1948) and Ursell (1950), has been calculated using a boundary-element method, as have the terms $O(\epsilon^2)$. In particular the results for $\psi_2^{(u)}$ confirm those previously obtained by Vada (1987), and McIver & McIver (1990). The time-independent part of the solution at $O(\epsilon^2)$, $\psi_2^{(s)}$, has not previously been discussed. From our present point of view these results represent the leading-order flow outside any boundary layers that form at the cylinder surface, and are considered as known.

Substituting (3.1) into (2.1) gives, at leading order,

$$\frac{\partial(\nabla^2\psi_1)}{\partial t} = 0, \tag{3.2}$$

and, as already indicated, the solution for ψ_1 is known. Since ψ_1 does not satisfy the no-slip boundary condition at the surface of the cylinder a boundary layer, the classical Stokes layer of thickness $O(\nu/\omega)^{1/2}$, is required. Accordingly we introduce Stokes-layer variables as

$$\Psi = \frac{R_s^{1/2}\psi}{\sqrt{2}\epsilon}, \qquad \rho = \frac{R_s^{1/2}(r-1)}{\sqrt{2}\epsilon}. \tag{3.3}$$

In the Stokes layer we expand the stream function in a manner similar to (3.1) as

$$\Psi = \epsilon\Psi_1(\rho,\theta,t) + \epsilon^2\{\Psi_2^{(u)}(\rho,\theta,t) + \Psi_2^{(s)}(\rho,\theta)\} + ... \tag{3.4}$$

Substituting (3.4) into the Stokes-layer equation gives, at leading order,

$$\frac{\partial}{\partial t}\left(\frac{\partial^2\Psi_1}{\partial\rho^2}\right) = \frac{1}{2}\frac{\partial^4\Psi_1}{\partial\rho^4}, \tag{3.5}$$

with boundary conditions

$$\Psi_1 = \frac{\partial\Psi_1}{\partial\rho} = 0 \quad \text{at } \rho = 0; \tag{3.6}$$

the required solution is

$$\Psi_1 = c_1(\theta)(\mathrm{e}^{\gamma_1\rho} - \gamma_1\rho - 1)\mathrm{e}^{\mathrm{i}t}, \tag{3.7}$$

where $\gamma_1 = -1 - \mathrm{i}$, and $c_1(\theta) = c_{11}(\theta) - \mathrm{i}c_{12}(\theta)$ is to be determined; the real part of any complex quantity is to be understood. The solution (3.7) is required to match the outer inviscid flow such that

$$\frac{\partial\Psi_1}{\partial\rho} \to \left.\frac{\partial\psi_1}{\partial r}\right|_{r=1} \quad \text{as } \rho \to \infty. \tag{3.8}$$

It proves convenient to write

$$\psi_1 = \psi_{11}(r,\theta)\cos t + \psi_{12}(r,\theta)\sin t, \quad \Psi_1 = \Psi_{11}(\rho,\theta)\cos t + \Psi_{12}(\rho,\theta)\sin t, \tag{3.9}$$

so that the matching requirement now gives

$$c_{11} = \frac{1}{2}\left[\frac{\partial\psi_{11}}{\partial r} - \frac{\partial\psi_{12}}{\partial r}\right]_{r=1}, \quad c_{12} = \frac{1}{2}\left[\frac{\partial\psi_{11}}{\partial r} + \frac{\partial\psi_{12}}{\partial r}\right]_{r=1}, \tag{3.10}$$

where the terms on the right-hand side of (3.10) are known from the inviscid solution of Riley & Yan (1996).

We turn next to the terms $O(\epsilon^2)$ in the Stokes-layer expansion (3.4). The time-dependent part $\Psi_2^{(u)}$ satisfies

$$\frac{1}{2}\frac{\partial^4 \Psi_2^{(u)}}{\partial \rho^4} - \frac{\partial}{\partial t}\left(\frac{\partial^2 \Psi_2^{(u)}}{\partial \rho^2}\right) = \left(\frac{\partial \Psi_1}{\partial \theta}\frac{\partial^3 \Psi_1}{\partial \rho^3} - \frac{\partial \Psi_1}{\partial \rho}\frac{\partial^3 \Psi_1}{\partial \rho^2 \partial \theta}\right)^{(u)}, \tag{3.11}$$

and the solution that satisfies the no-slip conditions

$$\Psi_2^{(u)} = \frac{\partial \Psi_2^{(u)}}{\partial \rho} = 0 \qquad \text{at } \rho = 0 \tag{3.12}$$

is

$$\Psi_2^{(u)} = \{c_{21}(\theta)\mathrm{e}^{\gamma_2 \rho} - c_1 c_1' \rho \mathrm{e}^{\gamma_1 \rho} + c_{22}(\theta)\rho + c_{23}(\theta)\}\mathrm{e}^{2\mathrm{i}t}, \tag{3.13}$$

where

$$\gamma_2 = -\sqrt{2}(1+\mathrm{i}), \quad c_{21}(\theta) = \frac{c_1 c_1' - c_{22}}{\gamma_2}, \quad c_{23}(\theta) = -c_{21}. \tag{3.14}$$

The solution (3.13) is required to match with the outer solution, so that

$$\frac{\partial \Psi_2^{(u)}}{\partial \rho} = \left.\frac{\partial \psi_2^{(u)}}{\partial r}\right|_{r=1} \qquad \text{as } \rho \to \infty. \tag{3.15}$$

If we write the known outer inviscid solution of Riley & Yan (1996) as

$$\psi_2^{(u)} = \psi_{21}(r,\theta)\cos 2t + \psi_{22}(r,\theta)\sin 2t, \tag{3.16}$$

then (3.13) requires

$$c_{22}(\theta) = \left.\frac{\partial \psi_{21}}{\partial r}\right|_{r=1} - \mathrm{i}\left.\frac{\partial \psi_{22}}{\partial r}\right|_{r=1}. \tag{3.17}$$

The remaining term within the Stokes layer at $O(\epsilon^2)$, the steady streaming $\Psi_2^{(s)}$, satisfies

$$\frac{\partial^4 \Psi_2^{(s)}}{\partial \rho^4} = 2\left(\frac{\partial \Psi_1}{\partial \theta}\frac{\partial^3 \Psi_1}{\partial \rho^3} - \frac{\partial \Psi_1}{\partial \rho}\frac{\partial^3 \Psi_1}{\partial \rho^2 \partial \theta}\right)^{(s)}. \tag{3.18}$$

The solution of (3.18) which satisfies the no-slip condition

$$\Psi_2^{(s)} = \frac{\partial \Psi_2^{(s)}}{\partial \rho} = 0 \quad \text{at } \rho = 0, \tag{3.19}$$

with $\partial \Psi_2^{(s)}/\partial \rho$ bounded as $\rho \to \infty$, is

$$\begin{aligned}\Psi_2^{(s)} = {} & [c_{11}c_{12}' - c_{12}c_{11}'][\tfrac{1}{4}\mathrm{e}^{-2\rho} - \rho \mathrm{e}^{-\rho}\cos\rho + 2\mathrm{e}^{-\rho}\sin\rho - \mathrm{e}^{-\rho}\cos\rho] \\ & + [c_{11}c_{11}' + c_{12}c_{12}'][\tfrac{1}{4}\mathrm{e}^{-2\rho} + 3\mathrm{e}^{-\rho}\cos\rho + \rho \mathrm{e}^{-\rho}\sin\rho + 2\mathrm{e}^{-\rho}\sin\rho] \\ & + c_{25}(\theta)\rho + c_{26}(\theta),\end{aligned} \tag{3.20}$$

where

$$\begin{aligned}c_{25}(\theta) &= \tfrac{3}{2}\left[-c_{11}c_{12}' + c_{12}c_{11}'\right] + \tfrac{3}{2}\left[c_{11}c_{11}' + c_{12}c_{12}'\right] \\ &= \frac{3}{4}\left\{\frac{\partial \psi_{11}}{\partial r}\left[\frac{\partial^2 \psi_{11}}{\partial r \partial \theta} - \frac{\partial^2 \psi_{12}}{\partial r \partial \theta}\right] + \frac{\partial \psi_{12}}{\partial r}\left[\frac{\partial^2 \psi_{11}}{\partial r \partial \theta} + \frac{\partial^2 \psi_{12}}{\partial r \partial \theta}\right]\right\},\end{aligned} \tag{3.21}$$

$$c_{26}(\theta) = \tfrac{3}{4}\left[c_{11}c'_{12} - c_{12}c'_{11}\right] - \tfrac{13}{4}\left[c_{11}c'_{11} + c_{12}c'_{12}\right]$$

$$= -\frac{13}{8}\left[\frac{\partial\psi_{11}}{\partial r}\frac{\partial^2\psi_{11}}{\partial r\partial\theta} + \frac{\partial\psi_{12}}{\partial r}\frac{\partial^2\psi_{12}}{\partial r\partial\theta}\right] + \frac{3}{8}\left[\frac{\partial\psi_{11}}{\partial r}\frac{\partial^2\psi_{12}}{\partial r\partial\theta} - \frac{\partial\psi_{12}}{\partial r}\frac{\partial^2\psi_{11}}{\partial r\partial\theta}\right]. \quad (3.22)$$

Since c_{25} is uniquely determined at this stage, the solution (3.20) cannot match directly with the outer, inviscid solution of Riley & Yan (1996). For $R_s \gg 1$, which is the case we consider in detail, an outer boundary layer is required for the transition from the Stokes layer to the outer inviscid flow. To proceed we continue to substitute the expansion (3.1) into (2.1) to give at $O(\epsilon^2)$, $O(\epsilon^3)$, $O(\epsilon^4)$ respectively

$$\frac{\partial(\nabla^2\psi_2^{(u)})}{\partial t} = 0, \quad (3.23)$$

$$\frac{\partial}{\partial t}(\nabla^2\psi_3) = \frac{1}{r}\frac{\partial(\psi_1, \nabla^2\psi_2^{(s)})}{\partial(r,\theta)} = \frac{1}{r}\left\{\frac{\partial(\psi_{11}, \nabla^2\psi_2^{(s)})}{\partial(r,\theta)}\cos t + \frac{\partial(\psi_{12}, \nabla^2\psi_2^{(s)})}{\partial(r,\theta)}\sin t\right\}, \quad (3.24)$$

$$\frac{1}{R_s}\nabla^4\psi_2^{(s)} = \frac{1}{r}\left[\frac{\partial(\nabla^2\psi_2^{(s)}, \psi_2^{(s)})}{\partial(r,\theta)} + \left\{\frac{\partial(\nabla^2\psi_3, \psi_1)}{\partial(r,\theta)}\right\}^{(s)}\right]. \quad (3.25)$$

The inviscid solution $\psi_2^{(u)}$ determined by Riley & Yan (1996) has already been employed in (3.15) above. However there is a correction to this due to the outflow from the Stokes layer, velocity $-\sqrt{2}c'_1(\theta)e^{it}/R_s^{1/2}$. But since our interest lies in the case $R_s \gg 1$ this is ignored, as is the contribution to $\Psi_2^{(u)}$ that results from it. Consider next equation (3.24) which we may integrate to give

$$\nabla^2\psi_3 = \frac{1}{r}\left\{\frac{\partial(\nabla^2\psi_2^{(s)}, \psi_{12})}{\partial(r,\theta)}\cos t - \frac{\partial(\nabla^2\psi_2^{(s)}, \psi_{11})}{\partial(r,\theta)}\sin t\right\} + \tilde{\phi}(r,\theta), \quad (3.26)$$

where $\tilde{\phi}(r,\theta)$ is an unknown function of r and θ only. We may use (3.26) to eliminate ψ_3 from (3.25) and write

$$\frac{1}{r}\left\{\frac{\partial(\nabla^2\psi_3, \psi_1)}{\partial(r,\theta)}\right\}^{(s)} = V_r^d\frac{\partial(\nabla^2\psi_2^{(s)})}{\partial r} + \frac{V_\theta^d}{r}\frac{\partial(\nabla^2\psi_2^{(s)})}{\partial\theta}, \quad (3.27)$$

where V_r^d, V_θ^d are the components of the Stokes drift velocity in the r- and θ-directions respectively, determined in terms of the known quantities ψ_{11} and ψ_{12}. Since our main concern is with the case $R_s \gg 1$, for which the viscous flow regime outside the Stokes layer is itself of boundary-layer character, we only require the form of the Stokes drift velocity close to the boundary. Accordingly we write

$$V_r^d = \left.\frac{\partial V_r^d}{\partial r}\right|_{r=1}(r-1) + \ldots, \qquad V_\theta^d = V_\theta^d|_{r=1} + \left.\frac{\partial V_\theta^d}{\partial r}\right|_{r=1}(r-1) + \ldots, \quad (3.28)$$

where

$$\left.\frac{\partial V_r^d}{\partial r}\right|_{r=1} = \frac{1}{2}\left\{\frac{\partial\psi_{12}}{\partial r}\frac{\partial^3\psi_{11}}{\partial r\partial\theta^2} - \frac{\partial\psi_{11}}{\partial r}\frac{\partial^3\psi_{12}}{\partial r\partial\theta^2}\right\}_{r=1}, \quad (3.29)$$

$$V_\theta^d|_{r=1} = \frac{1}{2}\left\{\frac{\partial\psi_{11}}{\partial r}\frac{\partial^2\psi_{12}}{\partial r\partial\theta} - \frac{\partial\psi_{12}}{\partial r}\frac{\partial^2\psi_{11}}{\partial r\partial\theta}\right\}_{r=1}, \quad (3.30)$$

may be evaluated from the known, leading-order inviscid solution. For $R_s \gg 1$ the

outer boundary layer has thickness $O(R_s^{-1/2})$, and is therefore thicker than the Stokes layer by a factor $O(\epsilon^{-1})$. Within it we write

$$r - 1 = R_s^{-1/2}\lambda, \qquad \psi_2^{(s)} = R_s^{-1/2}\tilde{\psi}_2^{(s)}, \tag{3.31}$$

so that, in terms of stream function and vorticity we have the boundary-layer equations

$$\left(V_\theta^d|_{r=1} + v_\theta^{(s)}\right)\frac{\partial\tilde{\omega}_2^{(s)}}{\partial\theta} + \left(\left.\frac{\partial V_r^d}{\partial r}\right|_{r=1}\lambda + v_\lambda^{(s)}\right)\frac{\partial\tilde{\omega}_2^{(s)}}{\partial\lambda} = \frac{\partial^2\tilde{\omega}_2^{(s)}}{\partial\lambda^2}, \tag{3.32}$$

$$\frac{\partial^2\tilde{\psi}_2^{(s)}}{\partial\lambda^2} = -\tilde{\omega}_2^{(s)}, \tag{3.33}$$

where

$$v_\theta^{(s)} = -\frac{\partial\tilde{\psi}_2^{(s)}}{\partial\lambda}, \qquad v_\lambda^{(s)} = \frac{\partial\tilde{\psi}_2^{(s)}}{\partial\theta}. \tag{3.34}$$

We note that in (3.32) the convective velocity for the vorticity is the Lagrangian mean velocity. At the inner edge of this outer boundary layer, $\lambda = 0$, we require

$$\tilde{\psi}_2^{(s)} = 0, \qquad v_\theta^{(s)} = -\left.\frac{\partial\Psi_2^{(s)}}{\partial\rho}\right|_{\rho=\infty} = -c_{25}(\theta) = V_i, \tag{3.35}$$

say, whilst at the outer edge, as $\lambda \to \infty$, we have

$$\tilde{\omega}_2^{(s)} \to 0, \qquad v_\theta^{(s)} \to -\left.\frac{\partial\psi_2^{(s)}}{\partial r}\right|_{r=1} = V_o, \tag{3.36}$$

say. These conditions must be supplemented by the periodicity condition $v_\theta^{(s)}|_{\theta=0} = v_\theta^{(s)}|_{\theta=2\pi}$, and similar for vorticity and stream function. Note also that the condition $v_\theta|_{\lambda=0} = V_i$ is used in the construction as a condition on the vorticity at $\lambda = 0$, by standard means. Both V_i and V_o may be calculated from the inviscid solution determined by Riley & Yan (1996). However, the boundary conditions (3.35) and (3.36) do not uniquely define the solution, since a potential vortex can be introduced. This difficulty has been encountered previously by Riley (1978) in a not dissimilar context, and by Riley (1981) in a different context. The resolution of the difficulty, which in the present case leads to a unique vortex strength, lies in the proper matching of the boundary-layer vorticity with the outer flow. To be sure, we have required $\tilde{\omega}_2^{(s)} \to 0$ at the edge of the boundary layer in (3.36); but this limit has to be achieved smoothly and we shall demonstrate this point in §4.

To supplement the condition on the streaming velocity $v_\theta^{(s)}$ at the edge of the boundary layer in (3.36) we require a potential-vortex contribution. Following Zapryanov, Kozhoukharova & Iordanova (1988) we adopt a system of bipolar coordinates (η, ζ) which are related to the Cartesian, (x, y), and polar, (r, θ), coordinates by

$$\left.\begin{aligned} x = r\cos\theta &= \frac{c\sin(\zeta+\zeta_0)}{\cosh\eta - \cos(\zeta+\zeta_0)}, \\ y = r\sin\theta &= \frac{c\sinh\eta}{\cosh\eta - \cos(\zeta+\zeta_0)} + h, \end{aligned}\right\} \tag{3.37}$$

where c and ζ_0 are constants to be determined such that $\zeta = 0$ coincides with $\theta = 0$

at $r = 1$, and $\eta = \eta_0$ corresponds to $r = 1$. This leads to

$$c = (h^2 - 1)^{1/2}, \quad \eta_0 = \cosh^{-1} h = -\ln\{h + (h^2 - 1)^{1/2}\}, \quad \zeta_0 = \sin^{-1}\{(h^2 - 1)^{1/2}/h\}. \tag{3.38}$$

In this coordinate system the stream function for the vortex located at $(x, y) = \{0, h - (h^2 - 1)^{1/2}\}$, ψ_v, is given by

$$\psi_v = -\frac{\Gamma \eta}{2\pi}, \tag{3.39}$$

The contribution which this makes to the velocity component $v_\theta^{(s)}$ at the edge of the boundary layer in (3.36) is

$$V_v = -\left.\frac{\partial \psi_v}{\partial r}\right|_{r=1} = \frac{\Gamma\{h - \cos(\zeta + \zeta_0)\}}{2\pi(h^2 - 1)^{1/2}}. \tag{3.40}$$

Before leaving this section we make two points. First we note that the differences between our analysis for the flow in this outer boundary layer, and that of Chaplin (1992), are that Chaplin does not include the contribution from the radial component of the drift velocity in the equation corresponding to (3.32) and his outer boundary condition corresponding to (3.36) is incomplete. Second we observe that both the outflow from the Stokes layer, and the presence of the vortex (3.39) will each affect our outer, inviscid, free-surface flow at $O(\epsilon^3)$.

4. Results and discussion

Before we describe our calculation method for the outer steady streaming boundary-layer flow, and assess the results from such calculations, we look at some of the ingredients that influence the flow. Consider first the boundary conditions (3.35) and (3.36). The velocities prescribed at $\lambda = 0$, and as $\lambda \to \infty$, clearly play a significant role in the dynamics of the boundary-layer flow. We note that the velocities V_i in (3.35), and V_o in (3.36), are both calculated from the inviscid solution of Riley & Yan (1996), the former indirectly through c_{25} in (3.21). We also note that $|V_i| \gg |V_o|$ and so we concentrate only on the former. However we note that the outer boundary condition must also be supplemented by a contribution from the potential vortex solution (3.40), for which the circulation Γ is not determined *a priori*. Consider V_i, as shown in figures 2(*a*), 2(*b*). In figure 2(*a*) the distribution of velocity at $r = 1$ when $h = 1.5$ for various values of k is shown, whilst in figure 2(*b*) the distribution for various cylinder depths with $k = 1$ is shown. These are typical, and there are two important points to note. The first is that the greatest activity is always at the top of the cylinder, at a point close to the free surface, as may be expected. The second is that the velocity is always negative, which indicates that the Reynolds stresses acting within the Stokes layer induce a negative circulation at the edge of it. Since the effect of V_o is small, and itself has no circulation, we may suppose that a negative circulation will be transmitted to the flow outside this outer boundary layer. Consider next the circulation induced outside the boundary layers by the bound vortex (3.39). The slip velocity induced by this at $r = 1$ is given by (3.40), and is shown in figure 3 for various values of h, with $\Gamma = 2\pi$. As may be anticipated, when the cylinder is close to the free surface high velocities are induced at the top of the cylinder $\theta = \frac{1}{2}\pi$. For large depths there is almost uniform flow at the cylinder surface. The value of Γ, for any particular situation, must be determined with care as discussed below. However, as we have argued above, we may expect Γ to be negative. Finally consider

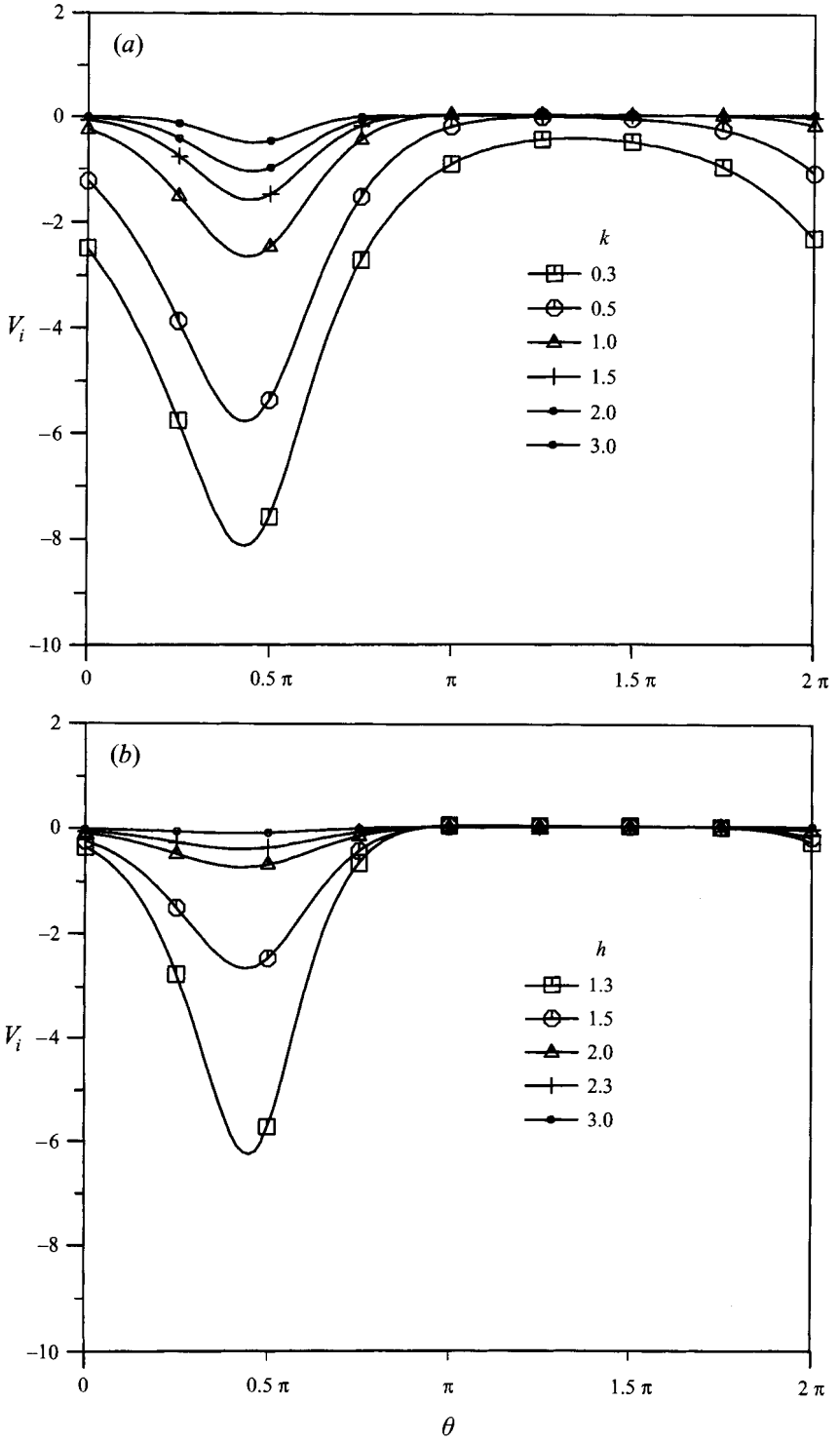

FIGURE 2. Velocity at the inner edge of the outer streaming boundary layer, (*a*) for different wavenumber k with depth $h = 1.5$, (*b*) for different depth h with wave number $k = 1.0$.

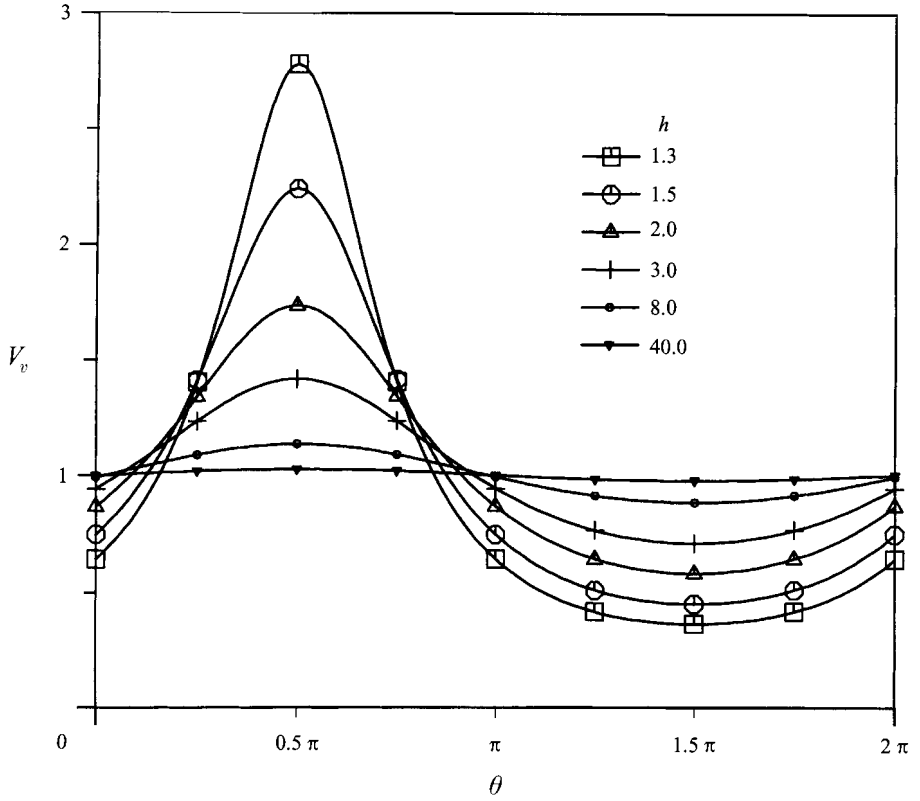

FIGURE 3. The slip velocity induced by the free-vortex flow at the surface of the cylinder, for different values of depth h with $\Gamma = 2\pi$.

the Stokes drift velocity. In (3.32) the θ-component, which enhances convection of vorticity in the θ-direction, is denoted by $V_\theta^d|_{r=1}$. This quantity is shown in figures 4(a), 4(b). In figure 4(a) we see the drift velocity for $h = 1.5$, when the cylinder is close to the free surface, for various values of k, whilst figure 4(b) shows the effect of increasing depth with $k = 1.0$. Again the greatest effect occurs at the point of closest approach of the cylinder to the free surface. We also note that in all cases the velocity is negative which implies that the Stokes drift velocity augments convection of vorticity in the clockwise sense. We also observe that as the wavenumber increases, or the depth increases, the effect of the Stokes drift diminishes. This trend is similar to that noted in relation to the tangential component of velocity at the edge of the Stokes layer, shown in figure 2.

We next consider the determination of a unique value for Γ, for given values of h and k. This is determined by a proper matching between the vorticity in the boundary layer with that outside it. Of course, in the present case, the flow outside the boundary layer is irrotational, but nevertheless to set $\tilde{\omega}_2^{(s)} = 0$ at $\lambda = \lambda_\infty$, where λ_∞ is the point chosen to represent the outer edge of the boundary layer in the computations, is not sufficient. We follow the approach of Riley (1981), where the flow outside the boundary layer was characterized by closed streamlines in a simply connected region, so that the inviscid outer flow was one of uniform vorticity. Define

$$\Omega(\Gamma, \lambda_\infty) = \int_0^{2\pi} \left| \frac{\partial \tilde{\omega}_2^{(s)}}{\partial \lambda} \right|_{\lambda=\lambda_\infty} \mathrm{d}\theta. \tag{4.1}$$

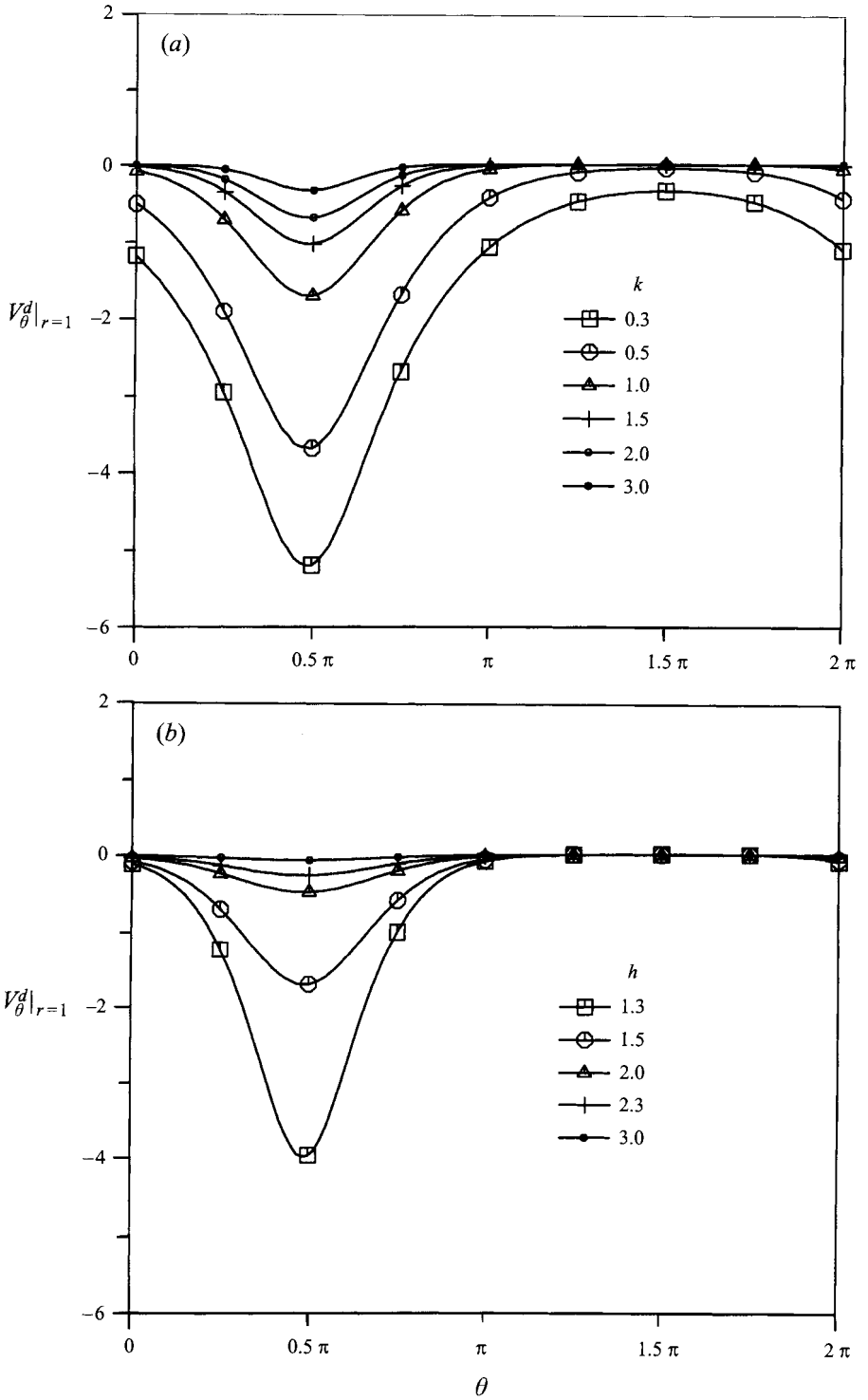

FIGURE 4. The Stokes drift velocity in the θ-direction at the surface of the cylinder (*a*) for different wavenumber k with depth $h = 1.5$, (*b*) for different depth h with wavenumber $k = 1.0$.

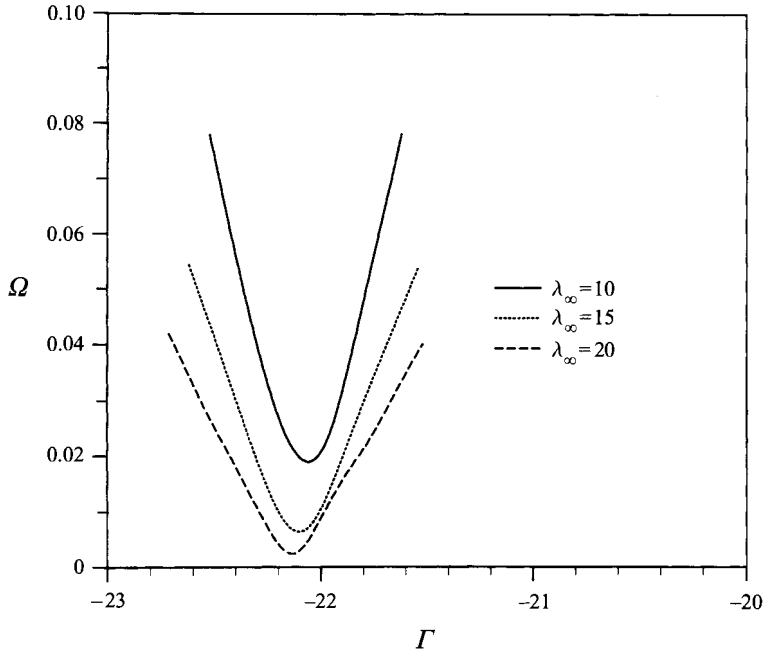

FIGURE 5. Variation of Ω with Γ for different values of λ_∞ and for $h = 1.5$, $k = 0.3$.

Riley demonstrates that, for a given λ_∞, we may expect Ω to pass through a minimum for some critical value of Γ, say Γ_c, and that as λ_∞ increases Γ_c becomes more sharply defined. To illustrate this we consider the case $h = 1.5, k = 0.3$ and in figure 5 we show the variation of Ω with Γ for various values of λ_∞. It is clear from this diagram that an accurate estimate of Γ_c can be made.

To integrate equations (3.32), (3.33) with the boundary conditions (3.35), (3.36) and the further condition of periodicity we use standard finite-difference techniques. Since, as we have already indicated, we anticipate that the steady streaming will be uni-directional, in a clockwise direction, we integrate equation (3.32) in the direction of θ decreasing. Derivatives in the streamwise direction are represented by second-order-accurate backward differences, whilst cross-stream derivatives are represented by central differences. For each pair of values h, k we must choose a suitable value of λ_∞ to represent the edge of the boundary layer. For the cases considered, λ_∞ lies in the range 10 to 25 with the larger values required for the larger values of h and k. In the discretized equations the mesh sizes varied, with $\delta\theta$ in the range $\pi/60$ to $\pi/40$, and $\delta\lambda$ in the range 0.05 to 0.1. In general the finer mesh was used for the smaller values of h and k. For a given h, k and suitably chosen values of λ_∞, $\delta\theta$ and $\delta\lambda$ the magnitude of the circulation outside the boundary layer, Γ_c, must be determined. To achieve this we first fix Γ and then integrate (3.32), (3.33) over the range $(2\pi, 0)$, using successive sweeps until the periodicity condition is satisfied. Varying Γ then allows us to minimize Ω, defined in (4.1), and so determine the appropriate value, Γ_c. Table 1 shows Γ_c for various values of h and k. The values of Γ_c shown in this table confirm our earlier predictions that the intensity of the streaming motion about the cylinder decreases as both the cylinder depth increases, and the wavelength of the incident wave decreases. We note that in the limiting case of large h and small k the flow will approximate a uniform orbital flow with $\Gamma_c = \Gamma_u = -6\pi e^{-2kh}$. The results of table 1 are not inconsistent with this, with the ratio Γ_c/Γ_u decreasing towards unity as we

$k \backslash h$	1.5	2.0	3.0
0.3	−22.11	−10.61	−4.76
1.0	−6.65	−2.19	-2.50×10^{-1}
2.0	−2.13	-3.71×10^{-1}	-2.41×10^{-3}
3.0	-9.40×10^{-1}	-3.51×10^{-2}	-1.10×10^{-4}

TABLE 1. The critical values of the circulation, Γ_c, for various values of h and k.

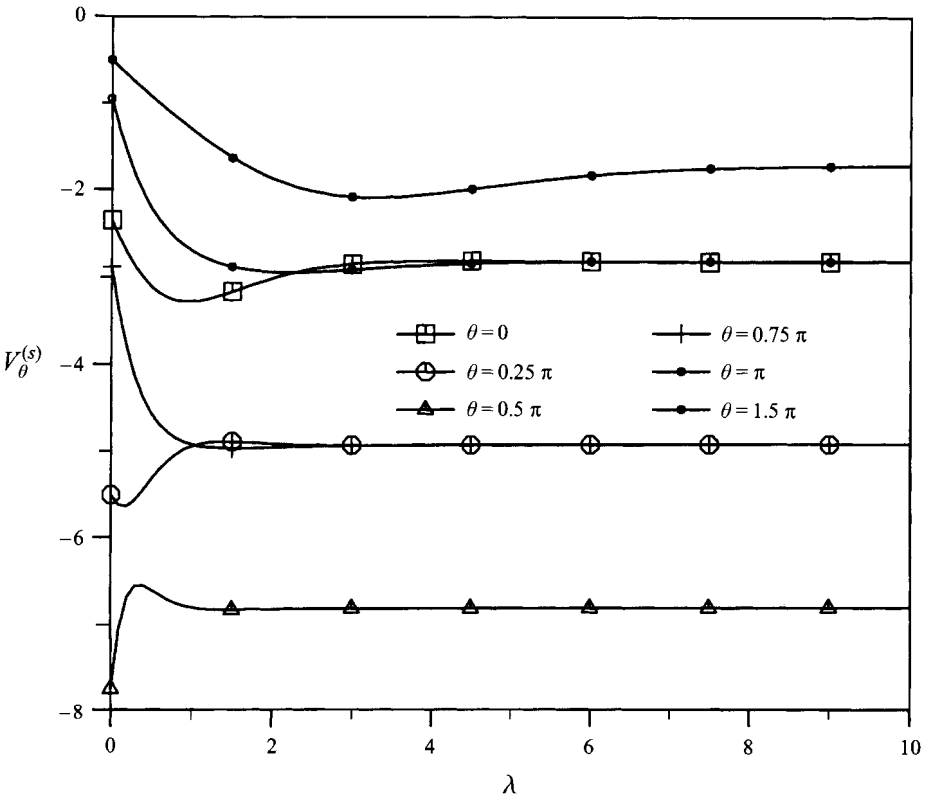

FIGURE 6. Velocity profiles for the tangential steady streaming in the outer boundary layer for $h = 1.5, k = 0.3$.

move out along the first row or up the last column. In figure 6 we show velocity profiles for the tangential steady streaming velocity in the outer boundary layer. This is for the case $h = 1.5, k = 0.3$ for which the steady streaming is quite vigorous. As we see, the flow is uni-directional in the clockwise direction. The profiles themselves are unremarkable; but the diagram does serve to illustrate the role of the outer boundary layer in adjusting the tangential velocity at the edge of the Stokes layer to the inviscid potential-vortex flow.

Next consider the force acting on the cylinder. For the normal stress we require the pressure. If a scale for this is taken as $\rho g a$, where ρ is the density, and g the acceleration due to gravity, then in the outer, inviscid, region we have Bernoulli's equation

$$p = -\tfrac{1}{2}k(v_r^2 + v_\theta^2) - k\frac{\partial \phi}{\partial t}, \tag{4.2}$$

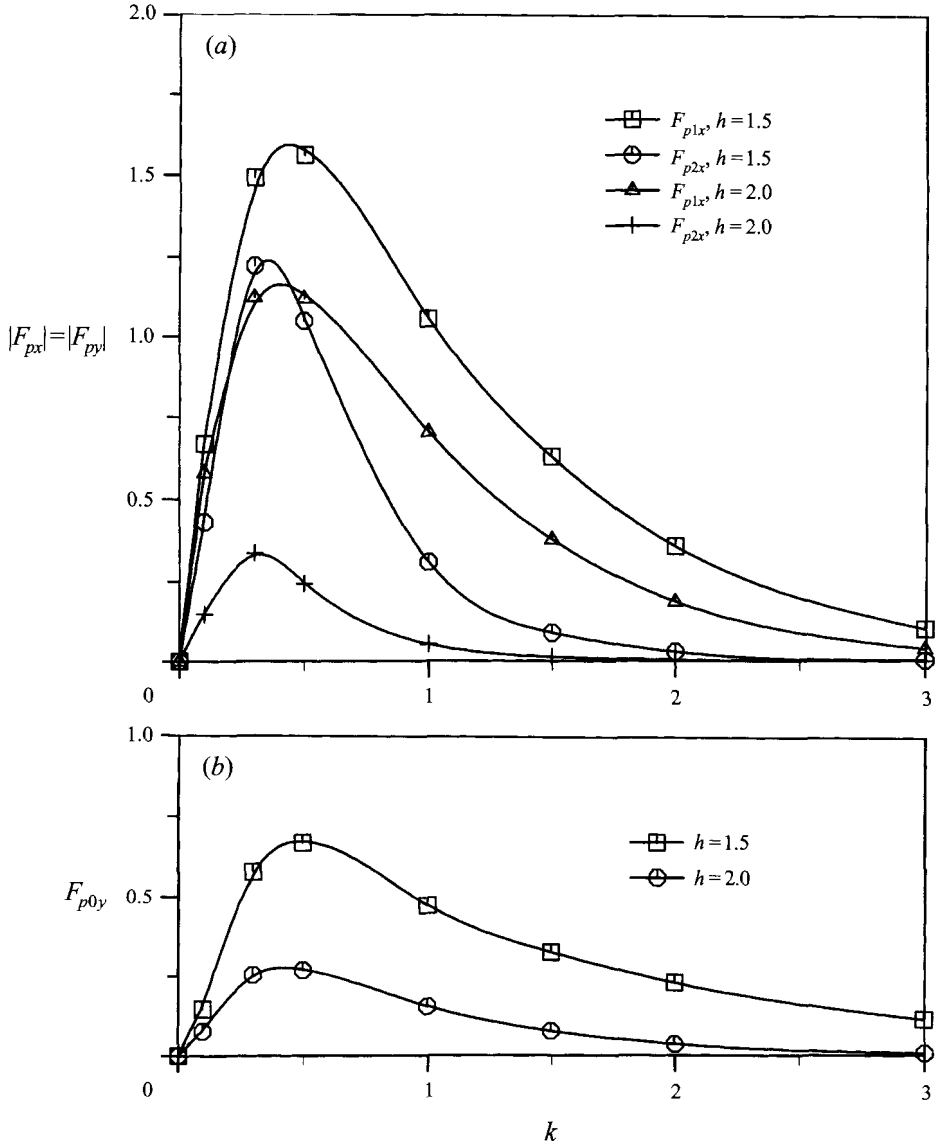

FIGURE 7. Force coefficients at the cylinder due to normal stresses (equation (4.3)) for $h = 1.5, 2.0$: (*a*) oscillatory force in the x- or y-direction, (*b*) mean vertical force.

where ϕ is the velocity potential. For $R_s \gg 1$, which is the case under consideration, this is the pressure transmitted to the cylinder surface through the thin boundary layers at it. For the basic inviscid flow we write (4.2) as

$$p = \epsilon(p_{11}\cos t + p_{12}\sin t) + \epsilon^2(p_{21}\cos 2t + p_{22}\sin 2t) + \epsilon^2 p_{02} + ..., \qquad (4.3)$$

where the coefficients p_{ij} depend only upon the spatial variables, and have been calculated by Riley & Yan (1996). There is a correction to the leading term of (4.3), with the fundamental frequency, due to outflow from the Stokes layer, $O(\epsilon^2/R_s^{1/2})$, and due to the presence of the vortex (3.39), $O(\epsilon^3)$. The latter also makes a contribution $O(\epsilon^4)$ to the time-averaged element of (4.3). The viscous component of the normal stress makes a contribution $O(\epsilon^3/R_s)$ to the leading term of (4.3). From these

	F_{pvx}			F_{pvy}		
$k\backslash h$	1.5	2.0	3.0	1.5	2.0	3.0
0.3	5.29	1.92	5.92×10^{-1}	7.16	2.24	6.34×10^{-1}
1.0	1.55	3.06×10^{-1}	1.33×10^{-2}	2.09	3.55×10^{-1}	1.42×10^{-2}
2.0	2.75×10^{-1}	1.82×10^{-2}	1.55×10^{-5}	3.67×10^{-1}	2.10×10^{-2}	1.64×10^{-5}
3.0	5.87×10^{-2}	4.70×10^{-4}	6.28×10^{-8}	7.84×10^{-2}	5.62×10^{-4}	6.65×10^{-8}

TABLE 2. The force coefficients F_{pvx} and F_{pvy} for various values of h and k.

corrections we calculate explicitly only the term $O(\epsilon^3)$, due to the presence of the vortex, since Chaplin (1984*b*) has detected a strong third-order component in his measurements of the fluctuating force. We denote this contribution to the pressure by

$$\epsilon^3(p_{v1}\cos t + p_{v2}\sin t). \tag{4.4}$$

Consider first the force on the cylinder due to the normal stresses obtained from (4.3). If we write this as $\boldsymbol{F}_p = (F_{px}, F_{py})$ then we have

$$F_{px} = \epsilon F_{p1x}\cos(t+\alpha_1) + \epsilon^2 F_{p2x}\cos(2t+\alpha_2) + \epsilon^2 F_{p0x} + ..., \tag{4.5}$$

with a similar expression for the y-component F_{py}. The phase angles α_i $(i = 1,2)$ have not been calculated. It is known, Vada (1987), that the force coefficients $|F_{pix}| = |F_{piy}|$ $(i = 1,2)$, and in figure 7(*a*) we show the force coefficients F_{pix} as a function of wavenumber k for varying h. The mean, or time-averaged horizontal force $F_{p0x} = 0$, however F_{p0y}, the time-averaged vertical force is non-zero and shown in figure 7(*b*). We note that all the force coefficients have a maximum close to $k = \frac{1}{2}$. The results shown in figure 7 agree with those presented by Vada, and are included here for completeness. We next consider the third-order normal stresses (4.4), due to the induced circulation about the cylinder, which make a contribution

$$\epsilon^3 F_{pvx}\cos(t+\alpha_{v1}), \qquad \epsilon^3 F_{pvy}\cos(t+\alpha_{v2}), \tag{4.6}$$

to the fluctuating force. F_{pvx}, F_{pvy} are shown in table 2 for the examples of table 1. As the cylinder approaches the free surface the relatively large numerical values of these quantities suggest that they will be detected in an experiment.

For the viscous shear stress we again choose $\rho g a$ as the scale so that the dimensionless shear stress, τ, may be written as

$$\tau R_s^{1/2}/\epsilon = -\frac{k}{\sqrt{2}}\left\{\epsilon\left(\frac{\partial^2\Psi_{11}}{\partial\rho^2}\cos t + \frac{\partial^2\Psi_{12}}{\partial\rho^2}\sin t\right) + \epsilon^2\left(\frac{\partial^2\Psi_{21}}{\partial\rho^2}\cos 2t + \frac{\partial^2\Psi_{22}}{\partial\rho^2}\sin 2t\right) + \epsilon^2\frac{\partial^2\Psi_{20}}{\partial\rho^2} + ...\right\}, \tag{4.7}$$

where $i = 1,2$, Ψ_{1i}, Ψ_{2i} are determined from (3.7) and (3.13) respectively and $\Psi_{20} = \Psi_2^{(s)}$ in (3.20). If the force on the cylinder due to the stress in (4.7) is denoted by $\boldsymbol{F}_v = (F_{vx}, F_{vy})$ then we have

$$F_{vx}R_s^{1/2}/\epsilon = \epsilon F_{v1x}\cos(t+\beta_1) + \epsilon^2 F_{v2x}\cos(2t+\beta_2) + \epsilon^2 F_{v0x} + ..., \tag{4.8}$$

with a similar expression for F_{vy}; the phase angles $\beta_i (i = 1,2)$ have not been calculated. The force coefficients F_{vix} and F_{viy}, $(i = 0,1,2)$, are shown in figures 8(*a*), 8(*b*) respectively. We again see that for these representative cases the force coefficients

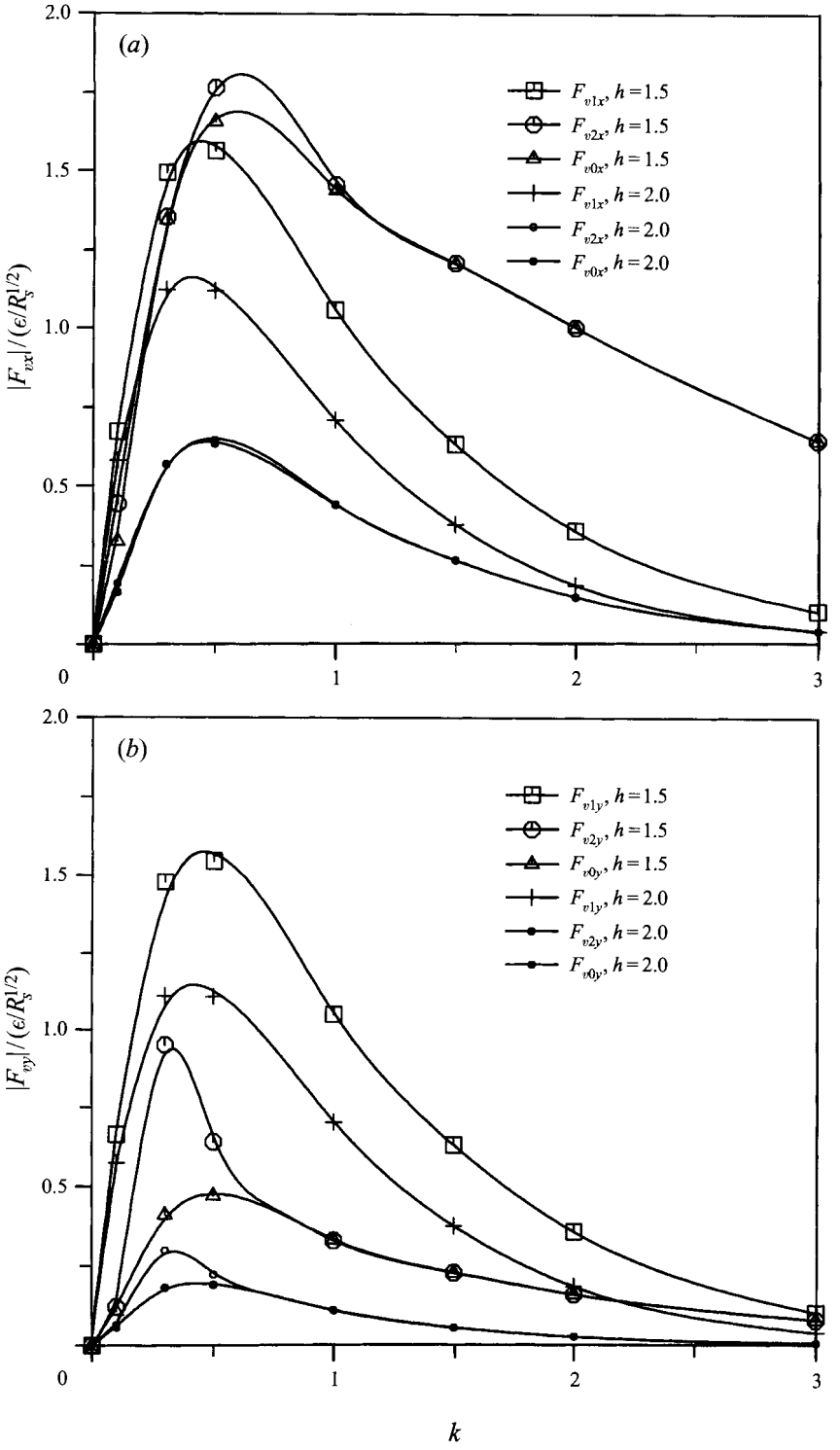

FIGURE 8. Force coefficients at the cylinder due to shear stresses for $h = 1.5, 2.0$: (*a*) in the x-direction, (*b*) in the y-direction.

exhibit maxima close to $k = \frac{1}{2}$. Note also that the time-averaged force components F_{v0x} and F_{v0y} are both non-zero. The latter enhances the mean lift coefficient, whilst the former yields a 'drag' force in the direction of wave propagation. A comparison of (4.5) and (4.8) shows that the viscous shear stress makes a contribution to the overall force on the cylinder that is less than the pressure force by a factor $O(\epsilon/R_s^{1/2})$.

The authors are indebted to the Marine Technology Directorate for financial support.

REFERENCES

CHAPLIN, J. R. 1984*a* Mass transport around a horizontal cylinder beneath waves. *J. Fluid Mech.* **140**, 175–187.

CHAPLIN, J. R. 1984*b* Nonlinear forces on a horizontal cylinder beneath waves. *J. Fluid Mech.* **147**, 449–464.

CHAPLIN, J. R. 1992 Orbital flow around a circular cylinder. Part 1. Steady streaming in non-uniform conditions. *J. Fluid Mech.* **237**, 395–411.

CHAPLIN, J. R. 1993 Orbital flow around a circular cylinder. Part 2. Attached flow at larger amplitudes. *J. Fluid Mech.* **246**, 397–418.

DEAN, W. R. 1948 On the reflexion of surface waves by a submerged circular cylinder. *Proc. Camb. Phil. Soc.* **44**, 483–491.

MCIVER, M. & MCIVER, P. 1990 Second-order wave diffraction by a submerged circular cylinder. *J. Fluid Mech.* **219**, 519–529.

RILEY, N. 1965 Oscillating viscous flows. *Mathematika,* **12**, 161–175.

RILEY, N. 1967 Oscillatory viscous flows: review and extension. *J. Inst. Maths Applics.* **3**, 419–434.

RILEY, N. 1971 Stirring of a viscous fluid. *Z. Angew Math. Phys.* **22**, 645–653.

RILEY, N. 1978 Circular oscillations of a cylinder in a viscous fluid. *Z. Angew Math. Phys.* **29**, 439–449.

RILEY, N. 1981 High Reynolds number flows with closed streamlines. *J. Engng Maths* **15**, 15–27.

RILEY, N. & YAN, B. 1996 Inviscid fluid flow around a submerged circular cylinder induced by free-surface travelling waves. *J. Engng Maths* (to be published).

STANSBY, P. K. & SMITH, P. A. 1991 Viscous forces on a circular cylinder in orbital flow at low Keulegan–Carpenter numbers. *J. Fluid Mech.* **229**, 159–171.

STUART, J. T. 1966 Double boundary layers in oscillatory viscous flow. *J. Fluid Mech.* **24**, 673–687.

URSELL, F. 1950 Surface waves on deep water in the presence of a submerged circular cylinder. I. *Proc. Camb. Phil. Soc.* **46**, 141–152.

VADA, T. A. 1987 A numerical solution of the second-order wave-diffraction problem for a submerged cylinder of arbitrary shape. *J. Fluid Mech.* **174**, 23–37.

WEHAUSEN, J. V. & LAITONE, E. V. 1960 Surface waves. In *Encyclopedia of Physics, Volume IX, Fluid Dynamics III* (ed. S. Flügge), pp. 446–778. Springer.

WU, G. X. 1991 On the second order wave reflection and transmission by a horizontal cylinder. *Appl. Ocean Res.* **13**, 58–62.

ZAPRYANOV, Z., KOZHOUKHAROVA, ZH. & IORDANOVA, A. 1988 On the hydrodynamic interaction of two circular cylinders oscillating in a viscous fluid. *Z. Angew Math. Phys.* **39**, 204–219.